Published in final edited form as:
Nat Struct Mol Biol. ; 19(2): . doi:10.1038/nsmb.2231.

Structural basis for autoinhibition and phosphorylation-dependent activation of c-Cbl

Hao Dou[#], **Lori Buetow**[#], **Andreas Hock**, **Gary J. Sibbet**, **Karen H. Vousden**, and **Danny T. Huang**
The Beatson Institute for Cancer Research, Garscube Estate, Switchback Road, Glasgow, G61 1BD, United Kingdom.

[#] These authors contributed equally to this work.

Abstract

Cbls are RING ubiquitin ligases that attenuate receptor tyrosine kinase (RTK) signal transduction. Cbl ubiquitination activity is stimulated by phosphorylation of a linker helix region (LHR) tyrosine residue. To elucidate the mechanism of activation, we determined structures of human CBL, a CBL–substrate peptide complex, and a phosphoTyr371-CBL–E2–substrate peptide complex, and compared them with the known structure of a CBL–E2–substrate peptide complex. Structural and biochemical analyses show that CBL adopts an autoinhibited RING conformation where the RING's E2-binding surface associates with CBL to reduce E2 affinity. PhosphoTyr371 activates CBL by inducing LHR conformational changes that eliminate autoinhibition, flip the RING domain and E2 into proximity of the substrate-binding site, and transform the RING domain into an enhanced E2-binding module. This activation is required for RTK ubiquitination. Our results present a mechanism for regulation of c-Cbl's activity by autoinhibition and phosphorylation-induced activation.

Keywords

c-Cbl; RING; E3; E2 binding; autoinhibition; conformational change; phosphorylation

Covalent attachment of ubiquitin (Ub) to proteins by sequential actions of Ub-activating enzyme (E1), Ub-conjugating enzyme (E2) and Ub ligase (E3) is an important cellular regulatory mechanism[1]. There are three classes of E3s (namely HECT, RING, and U-box[2,3]) that transfer Ub to substrate and thus play a pivotal role in determining substrate fate. Of those, RING E3s comprise the largest family, which can be subdivided into two classes: single-subunit and multi-protein complex. RING E3s function by recruiting an E2 thioesterified with Ub (E2~Ub) via the RING domain and substrate via a protein-protein interaction domain. The thioesterified Ub is then transferred directly from the E2 to a lysine side chain on the substrate. Much of our understanding of the regulation of RING E3s comes from studies of multi-protein RING complexes such as cullin-RING ligases (CRLs)[4,5]. Although both classes consist of about 300 members in the human genome[5,6], the mechanisms of single-subunit RING E3 regulation remain poorly understood.

Correspondence should be addressed to D.T.H. (d.huang@beatson.gla.ac.uk)..
Author contributions H.D., L.B., G.J.S. and D.T.H. designed, conducted and analyzed *in vitro* experiments. A.H. designed, conducted and analyzed *in vivo* experiments. K.H.V. designed and analyzed *in vivo* experiments. L.B. and D.T.H. wrote the manuscript. All authors discussed the results and commented on the manuscript.

Accession codes Coordinates and structure factors for the crystal structures of nCBL, CBL–S, E2–pCBL–S, E2–pCBL^{Y368F}–S and E2–pCBL$^{LHR–RING}$ have RCSB accession codes of 2Y1M, 2Y1N, 4A4C, 4A4B and 4A49, respectively.

Europe PMC Funders Author Manuscripts

Cbls (c-Cbl, Cbl-b and Cbl-c) are single-subunit RING E3s that negatively regulate a host of proteins by promoting their ubiquitination and subsequent degradation by the proteasome or via endocytosis[7–11]. Independent of their E3 activity, they also function as adaptors in a variety of diverse biological processes such as insulin signaling, bone resorption, and activation of mitogen-activated protein kinases[9,10]. Cbls act as both positive and negative regulators in the signal transduction of RTKs[10]: they propagate signals downstream of activated RTKs as adaptors and simultaneously ubiquitinate and promote degradation of the same RTKs as E3s. To carry out both of these roles, Cbls have evolved several protein-protein interaction modules. All Cbls share a highly conserved N-terminal SH2-containing tyrosine kinase-binding domain (TKBD), a LHR and a RING domain followed by a variable proline-rich region (PRR). In addition, c-Cbl and Cbl-b also contain a highly variable C-terminal extension involved in dimerization, binding of ubiquitinated proteins, and substrate recruitment following phosphorylation[9,12,13]. The TKBD mediates substrate specificity by binding to proteins containing phosphotyrosine motifs commonly found in RTKs or tyrosine kinases such as Zap-70 kinase[8,14,15] whereas the PRR recruits proteins containing an SH3 domain. The LHR and RING domain play central roles in recruiting E2s and in mediating target ubiquitination[7,16]. Mutations within these regions as observed in patients with myeloproliferative diseases and oncogenic forms of c-Cbl such as v-Cbl, 70ZCbl, and p95Cbl, abrogate c-Cbl's E3 activity[17–24].

Precise control of Cbls' E3 activity is required to facilitate its dual E3 and adaptor functions. Phosphorylation of a conserved tyrosine residue (Tyr371 in c-Cbl) within the LHR regulates Cbls' E3 activity[8,25,26]. Mass spectrometry studies show c-Cbl Tyr371 is phosphorylated in cells following epidermal growth factor (EGF) stimulation[27] and mutational analyses also demonstrate this event following insulin stimulation[28]. In addition, biochemical studies with Cbl fragments comprising the TKBD, LHR, and RING domain reveal that Cbls are more active ligases when phosphorylated[25,26], and mutation of c-Cbl Tyr371 abrogates RTK ubiquitination *in vivo*[8,20–22]. c-Cbl Tyr371 has recently emerged as one of the frequently mutated residues found in patients with myeloid neoplasms[24].

Although these studies support a role for Tyr371 phosphoregulation of c-Cbl's ligase activity, the existing structure of c-Cbl[16] does not explain how phosphorylation enhances ligase activity as Tyr371 is buried in the LHR-TKBD interface. Phosphorylation would disrupt this interface and likely perturb LHR-E2 interactions[16]. To understand how Tyr371 phosphorylation regulates c-Cbl's activity, we determined three new crystal structures of human CBL (also known as C-CBL): native CBL, CBL bound to ZAP-70 peptide, a TKBD substrate peptide, and CBL phosphorylated at Tyr371 in complex with the E2 UbcH5B and ZAP-70 peptide (referred to as nCBL, CBL–S and E2–pCBL–S, respectively). These structures and the existing structure of CBL bound to the E2 UbcH7 and ZAP-70 peptide[16] reveal dramatic conformational changes in the LHR and RING domain. In conjunction with biochemical analyses, we show that CBL adopts an autoinhibited conformation where its E2-binding surface on the RING domain is occluded in a competitive manner to reduce E2 binding, thereby attenuating its ligase activity. PhosphoTyr371 (pTyr371) activates CBL's E3 activity by inducing dramatic LHR conformational changes that (1) enhance overall E2-binding affinity by abolishing autoinhibition and modifying the E2-binding surface; and (2) place the RING domain and E2 in proximity of the TKBD substrate. These properties are required for EGF receptor (EGFR) ubiquitination.

Results

CBL structures reveal dramatic conformational changes

The structures of nCBL, CBL–S and E2–pCBL–S were determined using a CBL fragment ($CBL_{47–435}$) containing the N-terminal TKBD, LHR, and RING domain (Fig. 1 and Table

1). For discussion, the structural elements of the LHR are termed linker-loop 1 (LL1), linker-helix (LH), and linker-loop 2 (LL2) (Fig. 1a). The TKBD is similar in both our three structures and the structures of the TKBD alone or bound to ZAP-70 peptide[15] (r.m.s.d. between 0.4–1.4 Å for Cα atoms). The RING domain is also similar (r.m.s.d. between 0.45–0.53 Å for Cα atoms). Remarkably, the LHR appears extremely flexible: none of our LHR conformations resemble each other or the one observed in the existing structure of CBL bound to E2 and ZAP-70 substrate peptide[16] (E2–CBL–S; Fig. 1d), which results in dramatic changes in the orientation of the RING relative to the TKBD. In E2–CBL–S, the entire LHR packs against the TKBD; E2's catalytic cysteine is ~67 Å from ZAP-70 peptide and faces away from the substrate-binding site. In the phosphorylated complex, LH is released from the TKBD and the LHR undergoes ~180° rotation about LL1, reducing the gap between the E2's catalytic cysteine and ZAP-70 peptide to ~28 Å (Fig. 1e and Supplementary Fig. 1a).

nCBL (Fig. 1b) is more compact than E2–CBL–S; the RING-TKBD-LL2 interaction buries ~980 $Å^2$ of surface area. The LL1 and LH conformations are similar, but LL2 changes, which reorients the RING relative to the TKBD (Supplementary Fig. 1b). Notably, in nCBL, the E2-binding surface on the RING domain is now facing the TKBD. Upon binding to ZAP-70 peptide, LL2 assumes a new conformation and the RING domain undergoes ~70° rotation relative to that observed in nCBL, partially exposing the E2-binding surface on the RING domain (Fig. 1c and Supplementary Fig. 1b). Superposition of the RING domains from CBL–S and E2–CBL–S reveals a clash between E2 and the TKBD (Supplementary Fig. 1c), suggesting that further conformational changes of LL2 and rotation of the RING domain are necessary to accommodate an E2 (Fig. 1d).

CBL adopts autoinhibited and open conformations

In nCBL, the E2-binding surface on the RING domain directly contacts the TKBD in a manner that prevents E2 binding, revealing an autoinhibited conformation of the RING domain (Fig. 1b) hereby referred to as "closed". Surprisingly, the residues that maintain the closed conformation also engage in E2 binding as shown in E2–CBL–S (Fig. 2a,b). The closed RING conformation is stabilized by hydrophobic contacts involving Ile383, Trp408, and Phe418 from the RING domain and Leu219 and Met222 from the TKBD. In the structure of E2–CBL–S, Ile383, Trp408, and Phe418 bind directly to UbcH7 whereas Leu219 and Met222 assist Leu380 and Glu386 in creating a pocket to accommodate UbcH7's Arg5. Numerous hydrogen bonds involving residues from the RING domain, TKBD and LHR also stabilize the closed conformation; these residues are likewise involved in E2 binding.

Substrate binding and phosphorylation perturb the closed conformation (Fig. 1; see below). Binding of the TKBD substrate peptide induces slight movement within the TKBD and displaces the loop containing Phe271 ~4 Å towards LL2 (Fig. 2c). This disrupts the LL2-RING interactions seen in the closed RING conformation and establishes a new hydrophobic interaction between Phe271 and LL2's Phe378. These LL2 conformational changes rotate the RING domain into an open configuration. Structures of CBL's TKBD in complex with various phosphotyrosine substrate peptides show identical Phe271 displacement[29,30] and support the notion that binding of other substrates to the TKBD of CBL may induce partial RING opening.

To determine if the conformational changes observed in the structures occur in solution, we developed a disulfide assay to probe the proximity of the RING and TKB domains (see Supplementary Note and Supplementary Fig. 2). We engineered a disulfide pair with one residue in the RING domain (D435C) and one residue in the TKBD (R139C) such that their Cβs are within 7 Å in the nCBL structure, but widely separated in other CBL complex

structures (Fig. 3a). The constructed mutant, CBL R139C D435C, is referred to as diCys. Formation of a disulfide bond was monitored by SDS-PAGE, where disulfide-bonded diCys migrated faster than unmodified diCys (Fig. 3b,c). Wild-type CBL (WT) and individual Cys mutants did not form disulfide bonds. Addition of E2, ZAP-70 peptide or both impaired diCys disulfide bond formation consistent with the observed increased distances between Arg139 and Asp435 in CBL–S and E2–CBL–S.

RING-TKBD interaction competes against E2 binding

RING residues that maintain the TKBD interaction in nCBL also bind E2 in E2–CBL–S, implying that E2 binding is competitive. To probe the mode of autoinhibition, we introduced TKBD mutations that modify the affinity of the TKBD-RING interaction and assessed their effects. Previous structure-based studies of RING E3–E2 complexes reveal that RING domains recruit E2s via hydrophobic surfaces as observed in E2–CBL–S[16,31–33]. Each RING contains a critical residue on this surface that decreases E2 binding and hinders E3 activity when mutated[33,34]. This residue, Ile383, contacts Met222 in nCBL and UbcH7's Ala98 in E2–CBL–S (Fig. 3d). Substitution of Met222 to Phe or Glu should respectively enhance or weaken the hydrophobic interactions between the RING and TKBD in the closed conformation, thus modifying the rate of disulfide bond formation. Indeed, Phe substitution enhanced diCys disulfide bond formation, whereas Glu substitution reduced it (Fig. 3b,c).

Correspondingly, we tested the abilities of M222E and M222F mutants to bind UbcH5B using surface plasmon resonance analysis. The former displayed ~4-fold higher affinity for UbcH5B than WT, while the latter bound slightly weaker (Table 2 and Supplementary Fig. 3). Met222 forms part of UbcH7's Arg5 binding pocket in E2–CBL–S (Fig. 2b), so to control for the possibility of unintentional effects of an introduced electrostatic interaction, we mutated the corresponding residue in UbcH5B (Lys4) to alanine. Ala substitution reduced UbcH5B affinity, but the M222E mutant still exhibited ~3-fold higher affinity for UbcH5B K4A than WT (Table 2). Hence disruption of the RING-Met222 interaction augments E2 binding.

To determine whether the RING-TKBD interaction plays an inhibitory role on ligase activity, we performed Michaelis-Menten kinetic analyses on *in vitro* autoubiquitination assays using full-length M222E and M222F CBL mutants. Only catalytic efficiency (k_{cat}/K_m) was estimated because the reactions were not saturated at the highest achievable UbcH5B~Ub concentration. Compared to WT, CBL M222E displayed ~2.5-fold enhancement in k_{cat}/K_m whereas CBL M222F showed no appreciable differences (Table 3 and Supplementary Fig. 4a). Similar results were obtained using UbcH5B K4A or chain-terminating K0-Ub (Supplementary Fig. 4b,c). Addition of ZAP-70 peptide marginally increased CBL's UbcH5B-binding affinity (Table 2), but did not enhance autoubiquitination (Table 3). Together, these data support an autoinhibitory mechanism where the E2-binding surface on the RING domain associates with the TKBD to compete against E2 binding and thereby reduces CBL's catalytic efficiency.

pTyr371 enhances catalytic efficiency

We performed a kinetic analysis on CBL pY371 autoubiquitination to probe its effects on k_{cat}/K_m. Phosphorylation was achieved by co-expression of $CBL_{47–435}$ with a constitutively active Src construct (see Supplementary Methods). Unfortunately, we found trace amounts of CBL pY368 that were inseparable from CBL pY371. Despite this, CBL pY371 co-crystallized readily with UbcH5B and ZAP-70 peptide. To generate homogeneous pY371 for biochemical studies, we mutated Tyr368 to Phe. The structure of CBL Y368F pY371 bound to UbcH5B and ZAP-70 peptide (E2–$pCBL^{Y368F}$–S) was nearly identical to E2–pCBL–S (Table 1 and Supplementary Fig. 5a–c). In addition, CBL pY371 and Y368F

pY371 had similar kinetic constants for CBL autoubiquitination (Table 3 and Supplementary Fig. 6a); hence, Y368F substitution does not affect the structure or activity of CBL pY371.

Remarkably, both CBL pY371 and Y368F pY371 had ~1400-fold enhanced k_{cat}/K_m compared to WT (Table 3). Quantification of phosphorylation-induced changes in k_{cat} and K_m was not possible because the WT ubiquitination reaction could not be saturated; however, for this reaction our data are consistent with K_m and k_{cat} exceeding 43 μM and 0.0029 min^{-1}, respectively. In comparison, K_m (~7 μM) is decreased and k_{cat} (~ 0.7 min^{-1}) increased for CBL pY371 autoubiquitination; hence, changes in both k_{cat} and K_m contribute to the enhanced catalytic efficiency observed for CBL pY371 ubiquitination.

pTyr371 abolishes autoinhibition

In the structures of unphosphorylated CBL, LH's Tyr368 and Tyr371 "fasten" LH to the TKBD (Supplementary Fig. 7), but release upon Tyr371 phosphorylation (Fig. 1e). A phosphate moiety on Tyr371 cannot be accommodated in the observed conformation in the unphosphorylated CBL structures; hence we predicted that pTyr371 abolishes the ability of CBL to adopt the closed conformation. We probed disulfide bond formation of a diCys mutant harboring Y368F pY371 and found phosphorylation prevented disulfide bond formation (Fig. 3e), suggesting CBL no longer adopts the closed conformation. Based on our earlier finding, we also expected an increase in E2 binding with autoinhibitory disruption. Indeed, CBL Y368F pY371 enhanced UbcH5B binding by ~11-fold (Table 2), consistent with the decrease in K_m for autoubiquitination of CBL Y368F pY371 compared to WT.

Interestingly, unphosphorylated diCys Y368F formed disulfide bonds more slowly than diCys (Fig. 3e). Correspondingly, CBL Y368F marginally promoted UbcH5B binding (Table 2) and displayed ~2-fold enhancement in k_{cat}/K_m for CBL autoubiquitination (Table 3 and Supplementary Fig. 6b). Based on interactions observed in nCBL, this mutation likely weakens the LH-TKBD interactions and promotes RING opening, thereby augmenting activity. Mutations at Y371 cannot be phosphorylated and we predicted that Phe substitution might mimic unphosphorylated Tyr in preserving the closed conformation. We found that WT and CBL Y371F had comparable low catalytic efficiency (Table 3); CBL Y371F, however, had a slightly higher affinity for UbcH5B (Table 2), suggesting that Phe substitution marginally perturbs the LH-TKBD interaction in the closed conformation. Indeed, in our disulfide assay, diCys Y371F formed disulfide bonds more slowly than diCys (Fig. 3e). Thus, modifications and mutations to LH disrupt the closed, autoinhibited conformation; mutations such as Y368F and Y371F appear to shift the equilibrium to an open RING conformation, whereas phosphorylation abolishes the ability of CBL to adopt the closed conformation and thereby contributes to activation of CBL's ligase activity by reducing K_m for the reaction.

pTyr371-binding interface enhances E2 binding and activity

Closer inspection of E2–pCBL–S reveals that LH has flipped 180° about LL2 and rotated, thereby initiating contacts with the RING domain and E2 not present in E2–CBL–S (Figs. 1 and 4). In E2–pCBL–S, the C-terminus of LH abuts the N-terminal helix of E2. In addition, the tail of the RING domain has shifted to contact the N-terminus of LH. Because side-chain density was poor in the E2–pCBL–S map, detailed interactions are described based on a higher resolution structure of a complex of UbcH5B and a smaller fragment of phosphorylated CBL comprising the LHR and RING domains (residues 354–435) containing a Y368F mutation, referred to as E2–$pCBL^{LHR–RING}$ (Table 1, Fig. 4d–f and Supplementary Fig. 5d,e); the two structures have an r.m.s.d. of 1.1 Å for Cα atoms.

Key RING-E2 interactions as seen in E2–CBL–S and other RING–E2 complexes are unchanged[16,31,32] (Fig. 4c,f). pTyr371 does not directly bind UbcH5B, but instead sits in a pocket just below the E2-binding surface. The pocket is stabilized by hydrophobic interactions between pTyr371's aromatic ring and LL2's Leu370, Met374, and Phe378 and hydrophilic interactions between the phosphate moiety and Lys382 and Lys389 (Fig. 4f). New β-strands in LL1 and the C-terminal tail of the RING domain form a β-sheet that stabilizes pTyr371's binding pocket; the side chain of Val431 from the new RING β-strand forms a hydrophobic interaction with Phe378. Phe434 on the tail of the RING forms hydrophobic interactions with the aromatic group of Y368F.

To assess the importance of the pTyr371-binding interface on E2 binding and activity, we generated two CBL pY371 mutants, Y368F K389A and Y368F V431A to disrupt hydrogen bonding with the phosphate moiety of pTyr371 and destabilize hydrophobic interactions, respectively (Fig. 4f). Both mutants bound UbcH5B more weakly (Table 2) and had reduced k_{cat} and higher K_m values for CBL autoubiquitination than CBL Y368F pY371 (Table 3 and Supplementary Fig. 6a). To measure binding contributions originating from the pTyr371 LHR-RING conformation, we used the $CBL_{354–435}$ fragment containing only the LHR and RING domain and found that the pTyr371 fragment bound UbcH5B with two-fold higher affinity than the unphosphorylated counterpart and the fragment harboring a Y371F substitution (Table 2). Thus, Tyr371 phosphorylation also transforms the LHR and RING domain into a new conformation that enhances E2 binding and optimizes k_{cat} for CBL autoubiquitination.

pTyr371 is critical for EGFR ubiquitination

To determine whether abolishing autoinhibition and forming the pTyr371-binding interface are crucial for RTK ubiquitination, we employed *in vitro* and *in vivo* assays to probe the effects of our mutations on EGFR ubiquitination. Our *in vivo* assays were performed with full-length CBL and included EGF-stimulation to promote CBL Tyr371 phosphorylation; the Y371F, K389A and V431A mutants did not contain a Y368F substitution. Consistent with previous findings[8,20], CBL Y371F, which cannot abolish autoinhibition or form the pTyr371-binding interface, was defective in both *in vitro* and *in vivo* EGFR ubiquitination assays (Fig. 5a,b). Unphosphorylated CBL Y368F, which partially disrupts autoinhibition, also failed to promote EGFR ubiquitination *in vitro*. A previous mutagenesis study on the tail region of the RING domain identified Val431 and Phe434 as important residues for EGFR ubiquitination[35] but the mechanism was not established. CBLs harboring K389A or V431A substitutions and pY371 were defective in EGFR ubiquitination (Fig. 5a,b). Thus, both abolishing autoinhibition and forming the pTyr371-binding interface are required for ubiquitination of EGFR by CBL.

Discussion

E3s regulate the fates of thousands of targets involved in many cellular processes; hence precise control of their activity is vital. The E3 activity of c-Cbl, a single-subunit RING E3, is stimulated by Tyr371 phosphorylation, and while prior *in vitro* and *in vivo* studies clearly support phosphoregulation of c-Cbl's ligase activity via this Tyr[8,25,26], detailed mechanisms for this have been unavailable. Our results reveal an intricate regulation of c-Cbl's ligase activity by autoinhibition, conformational changes and phosphorylation.

Like Lipkowitz and co-workers[36], we propose a two-state model for the regulation of c-Cbl's activity (Fig. 5c–f). When unactivated, unphosphorylated c-Cbl exists in an equilibrium between an open, catalytically competent conformation and a closed, autoinhibited conformation. Phosphorylation of Y371 prohibits c-Cbl from accessing its closed conformation, thereby leading to a relative increase in activity or activated state. In

addition, the absence of the LH-TKBD contact enables dramatic movement of the RING domain, bringing E2 closer (~28 Å) to the TKBD substrate-binding site where full-length substrate may bridge the gap. pTyr371 also initiates new interactions within the LHR and RING domain that further enhance E2 binding and optimize ubiquitination activity.

Our kinetic analysis of CBL autoubiquitination shows that pTyr371 massively enhances CBL's catalytic efficiency by increasing k_{cat} and decreasing K_m. The improvement in k_{cat} may be attributed to E2~Ub positioning and optimization of the chemical environment of UbcH5B's active site in an analogous manner to Nedd8-modified CRL[37]. When unactivated, LL1's residues 354–359 do not make significant contact with other regions of CBL but their conformation is restricted by LH-TKBD interactions. Upon disruption of these interactions by pTyr371, this region may become flexible and promote juxtaposition of the RING domain and E2~Ub with lysines on CBL and Ub moieties of ubiquitinated CBL. Based on the 11-fold improvement in UbcH5B binding, we estimate that pTyr371 may improve the k_{cat} for CBL autoubiquitination at most by ~120-fold. A decrease in K_m value likely arises from enhancements observed in E2 binding due to elimination of autoinhibition and formation of the pTyr371-binding interface. Our data suggest that CBL Y368F pY371 has a stronger binding affinity for UbcH5B~Ub, the actual substrate, than UbcH5B: for any reaction, K_m is greater than K_d and approaches K_d only when the enzyme is in rapid equilibrium with the substrate. In our assay the K_m for CBL Y368F pY371 autoubiquitination (7.7 μM; Table 3) is lower than the K_d for UbcH5B binding (28 μM; Table 2). Thus thioesterified Ub may also contribute to the decrease in K_m value. However, we do not know if thioesterified Ub only promotes UbcH5B binding to activated CBL because we could not accurately determine K_m for WT CBL autoubiquitination. Consistent with our observation, Cdc34 esterified with Ub binds CRL with ~2-fold higher affinity than Cdc34 (ref. 37) and Ubc2~Ub binds E3α with ~7-fold higher affinity than Ubc2 (ref. 38). Further studies are required to elucidate how thioesterified Ub promotes E2 binding to a RING E3.

Tyr371 phosphorylation of CBL is required for ubiquitination of the TKBD substrate EGFR *in vivo* and promotes EGFR ubiquitination *in vitro*. Tyr371 phosphorylation does not play a significant role in substrate binding. We show that CBL Y368F pY371 only marginally increases the binding affinity for ZAP-70 peptide compared to WT CBL (Table 2), consistent with minimal structural changes in the ZAP-70 peptide binding site as observed in CBL–S, E2–CBL–S and E2–pCBL–S. Currently it is not known whether Tyr371 phosphorylation is a strict requirement for ubiquitination of every target. When unactivated, c-Cbl retains low activity where target ubiquitination can still occur *in vitro*, albeit at a much slower rate (Fig. 5b). Our results and previous Tyr371 mutational studies show that activated c-Cbl is required for ubiquitination of RTKs, Src and TRAIL receptors[8,20–22,39,40]. c-Cbl recruits targets via different modular domains and hence the location of target relative to the RING domain changes. Whether both states have preferences for target ubiquitination remains to be investigated.

A number of studies have identified mutations within c-Cbl's LHR and the RING domain in patients with myeloproliferative diseases; several of these mutations are sufficient to induce cell transformation (reviewed in[24]). Our data, together with the existing c-Cbl structure[16], provide new insights into how mutations, particularly in the LHR, can deregulate c-Cbl's activity (Supplementary Fig. 8). Mutations that perturb LH-TKBD interactions might change activity of the unactivated state by shifting the equilibrium. pTyr371-binding interface mutations might prevent proper ubiquitination of targets by impeding optimal ligase activity or exposing pTyr371 to rapid dephosphorylation. LHR mutations or deletions have the potential to affect the spatial arrangement of the RING domain and thus target

ubiquitination in both states. How these mutations contribute to oncogenicity requires further investigation.

Autoinhibition is a common mechanism in enzyme regulation[41]. Our data reveal a novel autoinhibitory mechanism where the E2-binding surface of the RING domain is blocked in a competitive manner. Prior to our study, it was not known whether the hydrophobic E2-binding surface on the RING domain could recognize other structural elements beside E2s. U-box E3s are structurally related to RING E3s and recruit E2s via a similar hydrophobic surface. CHIP U-box E3 is an asymmetric dimer where the E2-binding surface of one U-box domain is occluded while the other binds an E2 (ref. 42); no evidence suggests the occluded site becomes functional in binding an E2, whereas in c-Cbl, autoinhibition via the E2-binding surface is labile. Increasing numbers of RING E3s have been shown to be regulated by autoinhibition via different mechanisms[37,43–47]. We anticipate that future studies will reveal whether targeting the E2-binding surface of a RING domain via intra- or intermolecular interactions may be a common strategy in regulation of RING E3s.

We present the first molecular mechanism describing how phosphorylation regulates single-subunit RING E3 activity. Phosphorylation disrupts the LH-TKBD interaction, preventing c-Cbl from adopting any conformation accessible in the unactivated state. Other classes of E3s use similar regulatory mechanisms: for example, phosphorylation also promotes activity in the HECT E3 Itch by releasing the catalytic domain from autoinhibitory interactions[48]; for Smurf2, another HECT E3, binding of a partner protein performs the same function[49] and in CRL, post-translational modification with Nedd8 prevents inhibition by Cand1 (refs. 47,50). Phosphorylation also promotes flexibility and induces additional conformational changes that are essential for regulation of c-Cbl's E3 activity. When Tyr371 is unmodified, the RING domain is spatially restricted to regions distal from the TKBD substrate-binding site. Phosphorylation facilitates LHR conformational changes that enable the RING domain to approach the TKBD substrate-binding site. Given that Nedd8 modification of CRL also frees the Rbx1 RING domain to sample multiple orientations important for substrate polyubiquitination[47], we speculate that restricting and freeing the RING domain may be a general mechanism for regulating other RING E3s.

In conclusion, our results elucidate mechanisms for RING autoinhibition and phosphorylation-dependent activation of a single-subunit RING E3 and are supported by recent findings on Cbl-b[51]. These features may serve as a new paradigm for understanding the regulation of other RING E3s and modular enzymes.

Methods

Methods for protein preparation, *in vitro* and *in vivo* EGFR assays, mass spectrometry and structural determination are in the Supplementary Methods.

Crystallization

All crystals were obtained by mixing the proteins with equal volume of reservoir solution and grown by hanging drop vapor diffusion except where otherwise indicated. Crystals of nCBL ($CBL_{47–435}$; 13 mg ml^{-1}) were grown at 8°C in conditions containing 0.1 M Tris-HCl, pH 9.0–9.5, 3.7–4.0 M sodium formate and 5 mM DTT and flash-frozen in 0.1 M Tris-HCl, pH 9.0–9.5, 4.2 M sodium formate, 5 mM DTT, 8% (v/v) glycerol, 8% (v/v) ethylene glycol and 8% (w/v) sucrose. CBL–S was assembled by mixing $CBL_{47–435}$ (13 mg ml^{-1}) with ZAP-70 peptide (10 mM) at a 1:2.5 molar ratio, and crystals were grown at 18°C by sitting drop vapor diffusion in conditions containing 18–20% (w/v) PEG 3350 and 0.2 M ammonium formate. The crystals were flash-frozen in 22% (w/v) PEG 3350, 0.2 M ammonium formate, 8% (v/v) glycerol, 8% (v/v) ethylene glycol and 8% (w/v) xylitol. E2–

pCBL–S and E2–pCBL^{Y368F}–S were assembled by mixing $CBL_{47–435}$ pY371 or $CBL_{47–435}$ Y368F pY371 (8 mg ml^{-1}), respectively, with UbcH5B (23 mg ml^{-1}) and ZAP-70 peptide (10 mM) at a 1:1.2:2.5 molar ratio, and crystals were grown at 4°C in conditions containing 50 mM HEPES, pH 7.5, 0.2 M KCl and 31–35% (v/v) pentaerythritol propoxylate (5/4 PO/OH). The crystals were flash-frozen in the reservoir solution. E2–pCBL$^{LHR–RING}$ complex was assembled by mixing $CBL_{354–435}$ Y368F pY371 (5 mg ml^{-1}) with UbcH5B (8 mg ml^{-1}) at 1.2:1 molar ratio, and crystals were grown at 18°C by sitting drop vapor diffusion in conditions containing 20% (w/v) PEG 3350 and 0.2 M potassium thiocyanate. The crystals were flash-frozen in reservoir solution containing 20% (v/v) glycerol. Data were collected at beamline ID14–1 at ESRF and beamlines I02, I03 and I04–1 at DLS.

Disulfide crosslinking assays

$CBL_{47–435}$ variants (30 μg) were made up to 70 μl with 25 mM Tris-HCl (pH 7.6), 0.15 M NaCl and 1 mM DTT in the presence or absence of UbcH5B Cys to Ser mutant (100 μM), ZAP-70 peptide (20 μM) or both on ice. 0.8 μg of sample was removed for zero time point. The disulfide reactions were initiated by removal of DTT using a Zeba spin desalting column (Thermo Scientific) to exchange the buffer to 25 mM Tris-HCl (pH 7.6) and 0.15 M NaCl at room temperature (RT). 0.8 μg of sample was removed at indicated times, quenched with N-ethylmaleimide (NEM; 20 mM final concentration; Sigma) for 10 min and then mixed with 4X SDS loading buffer and resolved by SDS-PAGE. Alternatively, sodium tetrathionate (NaTT; 0.1 mM final concentration; Sigma) was added to the desalted CBL variant at RT for 5 min, quenched with NEM for 10 min and mixed with 4X SDS loading buffer. For thrombin cleavage reactions, NEM-treated samples were mixed with thrombin at RT for 90 min and stopped with 4X SDS loading buffer. Reduced samples were further prepared by adding 100 mM DTT. The gel was stained with SimplyBlue™ SafeStain (Invitrogen) and scanned on a densitometer (BioRAD GS-800). The volumes of the disulfide-bonded (D) and unmodified (U) species were quantified using Quantity One software (BioRAD). The fraction of disulfide bond formed (F) was expressed as F=D/(D+U). Reactions were performed in triplicate and curves for the fraction of disulfide bond formed over time were generated.

CBL autoubiquitination assay

Reactions were performed in 10 μl in 50 mM Tris-HCl (pH 7.6), 50 mM NaCl, 5 mM $MgCl_2$, 5 mM ATP, 1 mM DTT, 0.3 U ml^{-1} inorganic pyrophosphatase, 0.3 U ml^{-1} creatine kinase, 5 mM creatine phosphate, 2 mg ml^{-1} bovine serum albumin (BSA; for Supplementary Fig. 4 only), human UBA1 (0.5 μM), ^{32}P-Ub (80 μM) or ^{32}P-K0-Ub (70 μM), CBL variants (3 μM in Supplementary Fig. 4; 10 μM and 0.3 μM for unphosphorylated and phosphorylated CBL, respectively, in Supplementary Fig. 6) and indicated UbcH5B or UbcH5B K4A at 22°C (Supplementary Fig. 6a) or 30°C (Supplementary Figs. 4 and 6b). ZAP-70 peptide (0.2 mM) was included in the indicated reactions in Supplementary Fig. 4a. The reactions were initially incubated at 22°C or 30°C for 18 or 10 min, respectively, in the absence of CBL variants to charge E2 with ^{32}P-Ub. The highest achievable E2~Ub concentration was ~20 μM. The reactions were then initiated by addition of CBL variants, quenched with 2X SDS loading buffer containing 200 mM DTT at the indicated time, resolved by SDS-PAGE, dried and visualized by autoradiography or exposed to a phosphorimager and quantified using ImageQuant (GE Healthcare). All reported kinetic parameters were determined from initial rates by fitting two independent datasets to the Michaelis-Menten equation using SigmaPlot 8.0 (Systat Software Inc.). In this assay, the K_m value represents a combination of various Michaelis complexes (E2~Ub–CBL–different lysine residues on CBL or Ub_n–CBL).

E3-E2 and E3-substrate binding assay

CBL-E2 and CBL-ZAP-70 peptide binding experiments were performed at 25°C using a Biacore T100/T200 surface plasmon resonance (SPR) instrument with a CM-5 chip (Biacore Life Sciences) equilibrated in running buffer containing 25 mM Tris (pH 7.6), 150 mM NaCl, 0.1 mg ml^{-1} BSA, 1 mM DTT and 0.005% (v/v) Tween-20. Anti-GST was coupled onto a CM-5 chip and GST-CBL variants were captured to a level of ~1000-2000 RU for each experiment with GST or GST purified from Src co-expression as the control. Analytes were serially diluted in running buffer. Binding was measured between concentration ranges of 0–90 μM for E2 or ZAP-70 peptide analytes. For UbcH5B plus ZAP-70 peptide experiments, saturated ZAP-70 peptide (100 μM) was included in all E2 analytes (0–90 μM). Data reported are the difference in SPR signal between GST-CBL variants and GST alone. The data were analyzed globally by steady state affinity analysis using the Biacore T100 and T200 Evaluation software package (Biacore Life Sciences).

Supplementary Material

Refer to Web version on PubMed Central for supplementary material.

Acknowledgments

We would like to thank B. Schulman, F. Kozielski and A. Schuettelkopf for helpful discussions; V. Ulaganathan for computer support; S. Lilla and N. Morris for mass spectroscopic analyses; W. Clark and A. Keith for in-house DNA sequencing; Diamond Light Source (DLS) for access to beamlines I02, I03 and I04–1 (mx1229 and mx6683) that contributed to the results presented here; ID14–1 beamline at European Synchrotron Radiation Facility (ESRF) for access and synchrotron support. This work was supported by Cancer Research UK.

References

1. Hershko A, Ciechanover A. The ubiquitin system. Annu. Rev. Biochem. 1998; 67:425–79. [PubMed: 9759494]
2. Pickart CM, Eddins MJ. Ubiquitin: structures, functions, mechanisms. Biochim. Biophys. Acta. 2004; 1695:55–72. [PubMed: 15571809]
3. Dye BT, Schulman BA. Structural mechanisms underlying posttranslational modification by ubiquitin-like proteins. Annu. Rev. Biophys. Biomol. Struct. 2007; 36:131–50. [PubMed: 17477837]
4. Duda DM, Scott DC, Calabrese MF, Zimmerman ES, Zheng N, Schulman BA. Structural regulation of cullin-RING ubiquitin ligase complexes. Curr. Opin. Struct. Biol. 2011; 21:257–64. [PubMed: 21288713]
5. Deshaies RJ, Joazeiro CA. RING domain E3 ubiquitin ligases. Annu. Rev. Biochem. 2009; 78:399–434. [PubMed: 19489725]
6. Li W, et al. Genome-wide and functional annotation of human E3 ubiquitin ligases identifies MULAN, a mitochondrial E3 that regulates the organelle's dynamics and signaling. PLoS One. 2008; 3:e1487. [PubMed: 18213395]
7. Joazeiro CA, Wing SS, Huang H, Leverson JD, Hunter T, Liu YC. The tyrosine kinase negative regulator c-Cbl as a RING-type, E2-dependent ubiquitin-protein ligase. Science. 1999; 286:309–12. [PubMed: 10514377]
8. Levkowitz G, et al. Ubiquitin ligase activity and tyrosine phosphorylation underlie suppression of growth factor signaling by c-Cbl/Sli-1. Mol. Cell. 1999; 4:1029–40. [PubMed: 10635327]
9. Schmidt MH, Dikic I. The Cbl interactome and its functions. Nat. Rev. Mol. Cell. Biol. 2005; 6:907–18. [PubMed: 16227975]
10. Swaminathan G, Tsygankov AY. The Cbl family proteins: ring leaders in regulation of cell signaling. J. Cell. Physiol. 2006; 209:21–43. [PubMed: 16741904]

11. Yoon CH, Lee J, Jongeward GD, Sternberg PW. Similarity of sli-1, a regulator of vulval development in C. elegans, to the mammalian proto-oncogene c-cbl. Science. 1995; 269:1102–5. [PubMed: 7652556]
12. Peschard P, et al. Structural basis for ubiquitin-mediated dimerization and activation of the ubiquitin protein ligase Cbl-b. Mol. Cell. 2007; 27:474–85. [PubMed: 17679095]
13. Kozlov G, et al. Structural basis for UBA-mediated dimerization of c-Cbl ubiquitin ligase. J. Biol. Chem. 2007; 282:27547–55. [PubMed: 17635922]
14. Lupher ML Jr. Songyang Z, Shoelson SE, Cantley LC, Band H. The Cbl phosphotyrosine-binding domain selects a D(N/D]XpY motif and binds to the Tyr292 negative regulatory phosphorylation site of ZAP-70. J. Biol. Chem. 1997; 272:33140–4. [PubMed: 9407100]
15. Meng W, Sawasdikosol S, Burakoff SJ, Eck MJ. Structure of the amino-terminal domain of Cbl complexed to its binding site on ZAP-70 kinase. Nature. 1999; 398:84–90. [PubMed: 10078535]
16. Zheng N, Wang P, Jeffrey PD, Pavletich NP. Structure of a c-Cbl-UbcH7 complex: RING domain function in ubiquitin-protein ligases. Cell. 2000; 102:533–9. [PubMed: 10966114]
17. Andoniou CE, Thien CB, Langdon WY. Tumour induction by activated abl involves tyrosine phosphorylation of the product of the cbl oncogene. EMBO J. 1994; 13:4515–23. [PubMed: 7925293]
18. Blake TJ, Shapiro M, Morse HC 3rd, Langdon WY. The sequences of the human and mouse c-cbl proto-oncogenes show v-cbl was generated by a large truncation encompassing a proline-rich domain and a leucine zipper-like motif. Oncogene. 1991; 6:653–7. [PubMed: 2030914]
19. Bisson SA, Ujack EE, Robbins SM. Isolation and characterization of a novel, transforming allele of the c-Cbl proto-oncogene from a murine macrophage cell line. Oncogene. 2002; 21:3677–87. [PubMed: 12032836]
20. Thien CB, Walker F, Langdon WY. RING finger mutations that abolish c-Cbl-directed polyubiquitination and downregulation of the EGF receptor are insufficient for cell transformation. Mol. Cell. 2001; 7:355–65. [PubMed: 11239464]
21. Sanada M, et al. Gain-of-function of mutated C-CBL tumour suppressor in myeloid neoplasms. Nature. 2009; 460:904–8. [PubMed: 19620960]
22. Niemeyer CM, et al. Germline CBL mutations cause developmental abnormalities and predispose to juvenile myelomonocytic leukemia. Nat. Genet. 2009; 42:794–800. [PubMed: 20694012]
23. Grand FH, et al. Frequent CBL mutations associated with 11q acquired uniparental disomy in myeloproliferative neoplasms. Blood. 2009; 113:6182–92. [PubMed: 19387008]
24. Kales SC, Ryan PE, Nau MM, Lipkowitz S. Cbl and human myeloid neoplasms: the Cbl oncogene comes of age. Cancer Res. 2010; 70:4789–94. [PubMed: 20501843]
25. Kassenbrock CK, Anderson SM. Regulation of ubiquitin protein ligase activity in c-Cbl by phosphorylation-induced conformational change and constitutive activation by tyrosine to glutamate point mutations. J. Biol. Chem. 2004; 279:28017–27. [PubMed: 15117950]
26. Ryan PE, Sivadasan-Nair N, Nau MM, Nicholas S, Lipkowitz S. The N terminus of Cbl-c regulates ubiquitin ligase activity by modulating affinity for the ubiquitin-conjugating enzyme. J. Biol. Chem. 2010; 285:23687–98. [PubMed: 20525694]
27. Zhang Y, et al. Time-resolved mass spectrometry of tyrosine phosphorylation sites in the epidermal growth factor receptor signaling network reveals dynamic modules. Mol. Cell. Proteomics. 2005; 4:1240–50. [PubMed: 15951569]
28. Liu J, Kimura A, Baumann CA, Saltiel AR. APS facilitates c-Cbl tyrosine phosphorylation and GLUT4 translocation in response to insulin in 3T3-L1 adipocytes. Mol. Cell. Biol. 2002; 22:3599–609. [PubMed: 11997497]
29. Hu J, Hubbard SR. Structural characterization of a novel Cbl phosphotyrosine recognition motif in the APS family of adapter proteins. J. Biol. Chem. 2005; 280:18943–9. [PubMed: 15737992]
30. Ng C, Jackson RA, Buschdorf JP, Sun Q, Guy GR, Sivaraman J. Structural basis for a novel intrapeptidyl H-bond and reverse binding of c-Cbl-TKB domain substrates. EMBOJ. 2008; 27:804–16. [PubMed: 18273061]
31. Dominguez C, Bonvin AM, Winkler GS, van Schaik FM, Timmers HT, Boelens R. Structural model of the UbcH5B/CNOT4 complex revealed by combining NMR, mutagenesis, and docking approaches. Structure. 2004; 12:633–44. [PubMed: 15062086]

32. Mace PD, et al. Structures of the cIAP2 RING domain reveal conformational changes associated with ubiquitin-conjugating enzyme (E2) recruitment. J. Biol. Chem. 2008; 283:31633–40. [PubMed: 18784070]
33. Brzovic PS, et al. Binding and recognition in the assembly of an active BRCA1/BARD1 ubiquitin-ligase complex. Proc. Natl. Acad. Sci. USA. 2003; 100:5646–51. [PubMed: 12732733]
34. Buchwald G, van der Stoop P, Weichenrieder O, Perrakis A, van Lohuizen M, Sixma TK. Structure and E3-ligase activity of the Ring-Ring complex of polycomb proteins Bmi1 and Ring1b. EMBO J. 2006; 25:2465–74. [PubMed: 16710298]
35. Visser Smit GD, et al. Cbl controls EGFR fate by regulating early endosome fusion. Sci. Signal. 2009; 2:ra86. [PubMed: 20029031]
36. Ryan PE, Davies GC, Nau MM, Lipkowitz S. Regulating the regulator: negative regulation of Cbl ubiquitin ligases. Trends Biochem. Sci. 2006; 31:79–88. [PubMed: 16406635]
37. Saha A, Deshaies RJ. Multimodal activation of the ubiquitin ligase SCF by Nedd8 conjugation. Mol. Cell. 2008; 32:21–31. [PubMed: 18851830]
38. Siepmann TJ, Bohnsack RN, Tokgoz Z, Baboshina OV, Haas AL. Protein interactions within the N-end rule ubiquitin ligation pathway. J. Biol. Chem. 2003; 278:9448–57. [PubMed: 12524449]
39. Song JJ, et al. c-Cbl-mediated degradation of TRAIL receptors is responsible for the development of the early phase of TRAIL resistance. Cell. Signal. 2010; 22:553–63. [PubMed: 19932172]
40. Yokouchi M, et al. Src-catalyzed phosphorylation of c-Cbl leads to the interdependent ubiquitination of both proteins. J. Biol. Chem. 2001; 276:35185–93. [PubMed: 11448952]
41. Pufall MA, Graves BJ. Autoinhibitory domains: modular effectors of cellular regulation. Annu. Rev. Cell. Dev. Biol. 2002; 18:421–62. [PubMed: 12142282]
42. Zhang M, et al. Chaperoned ubiquitylation--crystal structures of the CHIP U box E3 ubiquitin ligase and a CHIP-Ubc13-Uev1a complex. Mol. Cell. 2005; 20:525–38. [PubMed: 16307917]
43. Du F, Navarro-Garcia F, Xia Z, Tasaki T, Varshavsky A. Pairs of dipeptides synergistically activate the binding of substrate by ubiquitin ligase through dissociation of its autoinhibitory domain. Proc. Natl. Acad. Sci. USA. 2002; 99:14110–5. [PubMed: 12391316]
44. Lopez J, et al. CARD-mediated autoinhibition of cIAP1's E3 ligase activity suppresses cell proliferation and migration. Mol. Cell. 2011; 42:569–83. [PubMed: 21549626]
45. Chaugule VK, et al. Autoregulation of Parkin activity through its ubiquitin-like domain. EMBO J. 2011; 30:2853–67. [PubMed: 21694720]
46. Yamoah K, Oashi T, Sarikas A, Gazdoiu S, Osman R, Pan ZQ. Autoinhibitory regulation of SCF-mediated ubiquitination by human cullin 1's C-terminal tail. Proc. Natl. Acad. Sci. USA. 2008; 105:12230–5. [PubMed: 18723677]
47. Duda DM, Borg LA, Scott DC, Hunt HW, Hammel M, Schulman BA. Structural insights into NEDD8 activation of cullin-RING ligases: conformational control of conjugation. Cell. 2008; 134:995–1006. [PubMed: 18805092]
48. Gallagher E, Gao M, Liu YC, Karin M. Activation of the E3 ubiquitin ligase Itch through a phosphorylation-induced conformational change. Proc. Natl. Acad. Sci. USA. 2006; 103:1717–22. [PubMed: 16446428]
49. Wiesner S, et al. Autoinhibition of the HECT-type ubiquitin ligase Smurf2 through its C2 domain. Cell. 2007; 130:651–62. [PubMed: 17719543]
50. Goldenberg SJ, et al. Structure of the Cand1-Cul1-Roc1 complex reveals regulatory mechanisms for the assembly of the multisubunit cullin-dependent ubiquitin ligases. Cell. 2004; 119:517–28. [PubMed: 15537541]
51. Kobashigawa Y, Tomitaka A, Kumeta H, Noda NN, Yamaguchi M, Inagaki F. Autoinhibition and phosphorylation-induced activation mechanisms of human cancer and autoimmune disease-related E3 protein Cbl-b. Proc. Natl. Acad. Sci. USA. 2011

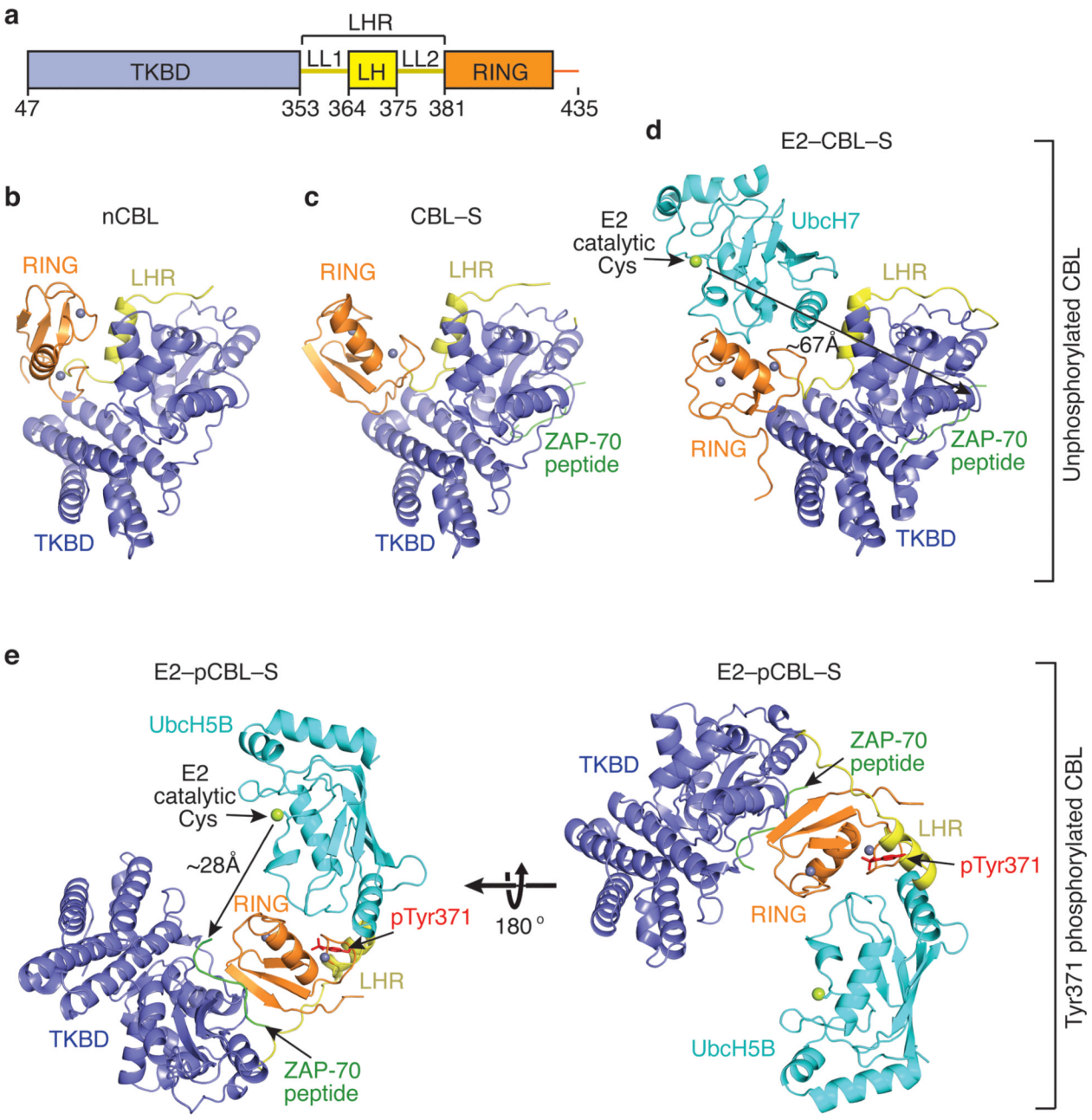

Figure 1.

Ensemble of CBL structures. (**a**) Diagram of the crystallized CBL fragment: TKBD in blue, LHR (LL1, LH and LL2) in yellow and RING domain in orange. Residues encompassing each domain are indicated. All structures are colored as in **a** and oriented as in **b**. Zn^{2+} atoms are depicted as grey spheres, ZAP-70 peptide is green and E2 is cyan with its catalytic cysteine shown as a lime sphere. Phosphorylation state is indicated on the right. (**b**) nCBL structure. (**c**) CBL–S structure. (**d**) E2–CBL–S structure (PDB 1FBV[16]). The measured gap between the E2's catalytic cysteine and TKBD substrate peptide is shown by the arrows here

and in **e**. (**e**) E2–pCBL–S structure. Right panel is in the same orientation as **b** and left panel is rotated by 180° about the x-axis. pTyr371 side chain is shown in red.

Europe PMC Funders Author Manuscripts

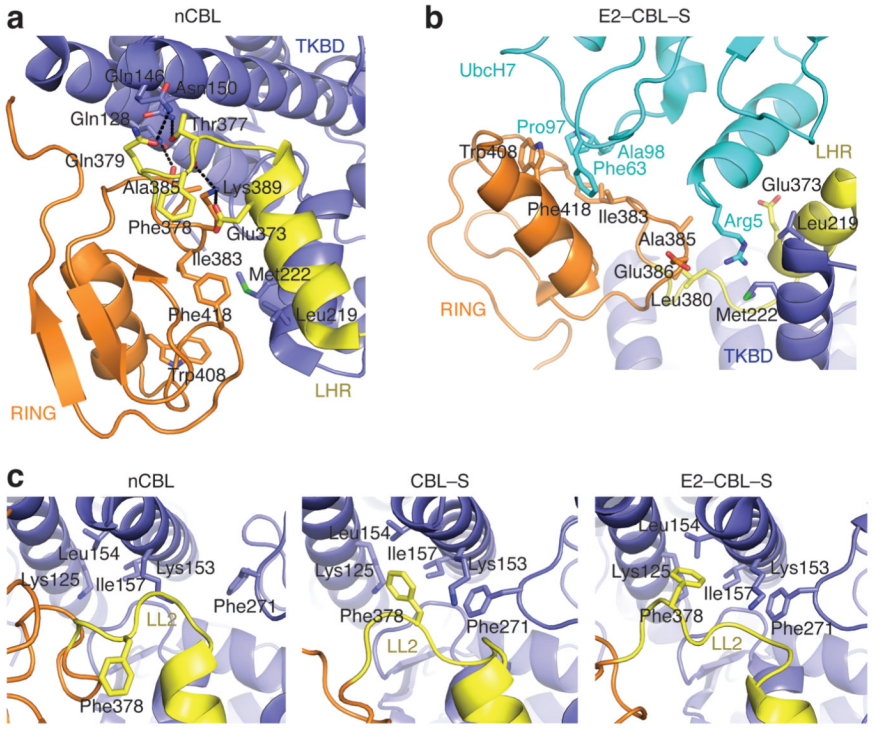

Figure 2.

CBL autoinhibition via the E2-binding site. (**a**) Interactions in nCBL that stabilize the closed conformation. (**b**) Interactions in E2–CBL–S involved in CBL-E2 binding. (**c**) The LL2 conformations in nCBL (left), CBL–S (middle), and E2–CBL–S (right). All panels are colored as in Fig. 1.

Europe PMC Funders Author Manuscripts

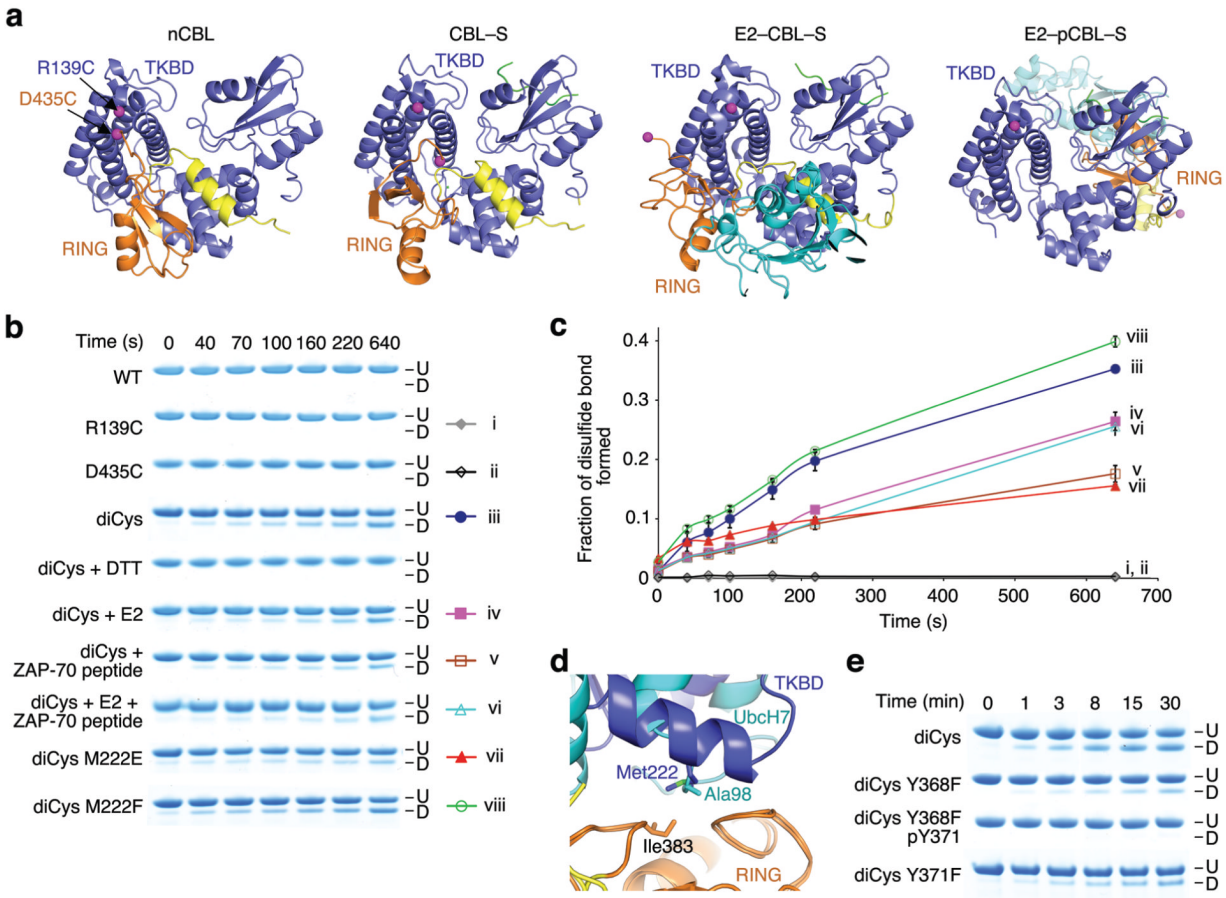

Figure 3.

The RING domain adopts different conformations in solution. (**a**) Structures of nCBL (left), CBL–S (middle left), E2–CBL–S (middle right) and E2–pCBL–S (right) colored as in Fig. 1 with TKBD's Arg139 and RING's Asp435 displayed as magenta spheres. Phe434 is displayed in E2–CBL–S because Asp435 is absent. (**b**) SDS-PAGE showing disulfide bond formation for unphosphorylated $CBL_{47–435}$ variants in the absence or presence of E2, ZAP-70 peptide or both. Disulfide-bonded (D) and unmodified (U) species are indicated. The color symbols on the right with Roman numerals correspond to the chart legend in **c**. (**c**) Plots for fraction of disulfide bond formed over time for CBL variants in **b**. Curves are indicated with symbols and corresponding Roman numerals in **b**. Triplicate reactions were performed and the s.e.m. are shown. (**d**) Superposition of the RING domains from nCBL and E2–CBL–S. Coloring is as described in Fig. 1. (**e**) SDS-PAGE showing disulfide bond formation for diCys variants with or without Tyr371 phosphorylation. Labels are as in **b**.

Europe PMC Funders Author Manuscripts

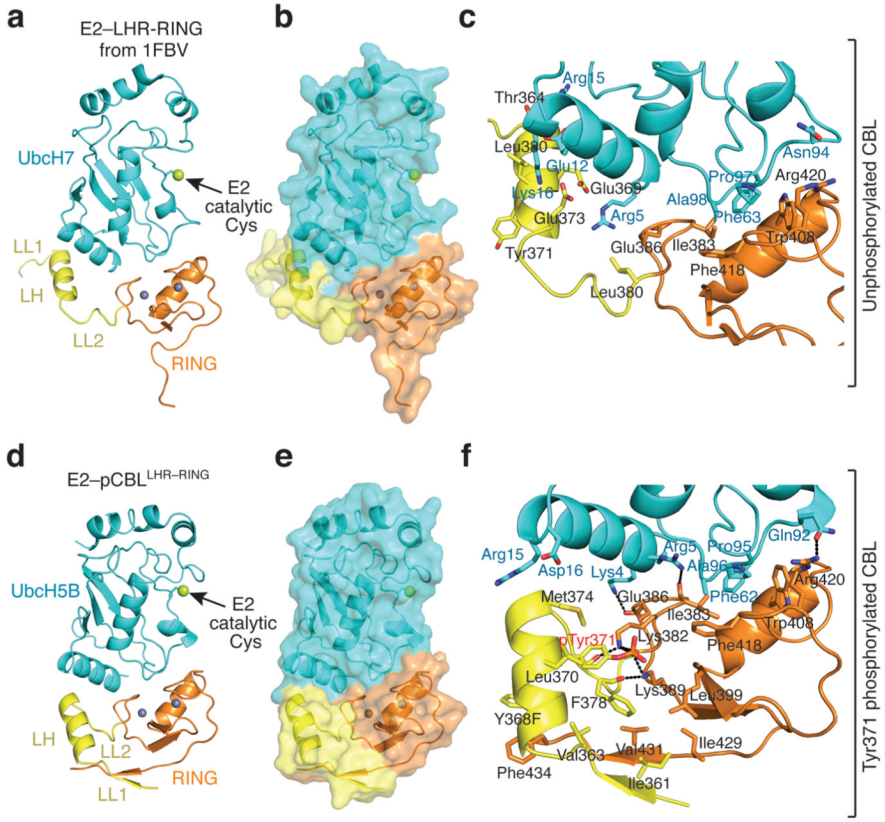

Figure 4.

pTyr371 alters LHR conformation and interactions. All coloring is as described in Fig. 1. Phosphorylation state is indicated on the right. (**a**) E2-LHR-RING portion of structure from E2–CBL–S (PDB 1FBV[16]). (**b**) Surface representation of **a**. (**c**) Close up view of the interactions between UbcH7 and LHR-RING domain in E2–CBL–S. (**d**) Structure of E2–pCBL$^{LHR–RING}$. (**e**) Surface representation of **d**. (**f**) Close up view of the pTyr371-binding site and UbcH5B-binding interface in E2–pCBL$^{LHR–RING}$.

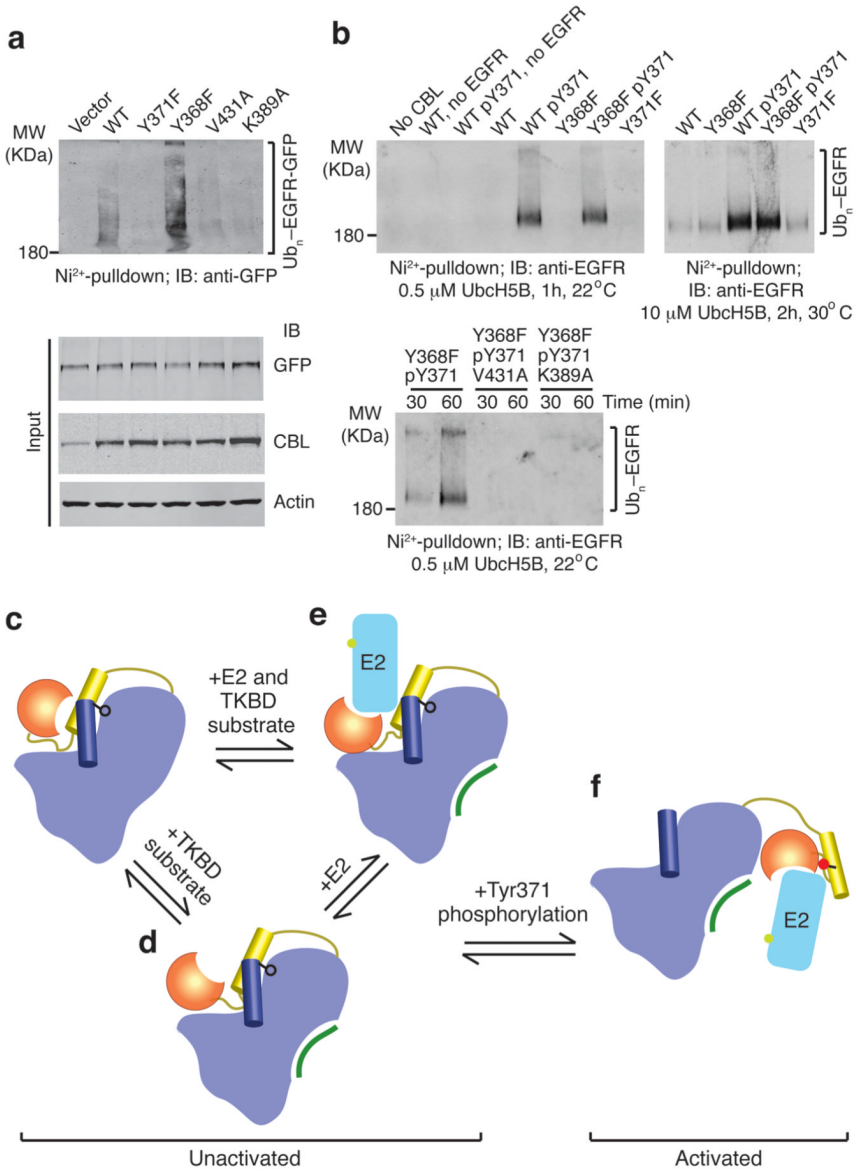

Figure 5.

EGFR ubiquitination by CBL. (**a**) Immunoblots from *in vivo* EGFR ubiquitination by full-length CBL variants. Ni^{2+}-pulldown products were Western blotted for GFP to detect His-Ub-EGFR-GFP. Protein input levels were assessed with the indicated antibodies. (**b**) Western blots from *in vitro* EGFR ubiquitination by CBL47–435 variants. Ni^{2+}-pulldown products were Western blotted for EGFR to detect His-Ub-EGFR. (**c**–**f**) Model for autoinhibition and phosphorylation-dependent activation of c-Cbl. c-Cbl exists in an unactivated state (**c**–**e**) where its E2-binding affinity is reduced by a competitive RING autoinhibitory mechanism. Coloring of c-Cbl, E2 and substrate is as in Fig. 1. (**c**) In the absence of E2, c-Cbl adopts a closed conformation where the RING's E2-binding surface associates with the TKBD. (**d**) TKBD substrate binding induces partial RING opening. (**e**) E2 binding causes the RING domain to adopt an open conformation. The TKBD competes against E2 for RING binding, reducing E2 affinity and E3 activity. In the unactivated state, Tyr371 (black ball-and-stick) secures the LH to the TKBD and limits the RING domain

rotation to a region distal from the TKBD substrate-binding site. (**f**) pTyr371 (red ball-and-stick) activates c-Cbl by releasing LH from the TKBD, thereby abolishing autoinhibition, altering LH-RING-E2 interactions and promoting dramatic LHR conformational changes that bring the RING domain and E2 into proximity of substrate.

Europe PMC Funders Author Manuscripts

Europe PMC Funders Author Manuscripts

Table 1

Data collection and refinement statistics

	nCBL	CBL–S	E2–pCBL–S	E2–pCBL^{Y368F}–S	E2–pCBL$^{LHR–RING}$
Data collection					
Space group	$C222_1$	$P6_5$	$P6_522$	$P6_522$	$P3_221$
Cell dimensions					
a, *b*, *c* (Å)	146.8, 146.8, 348.2	93.6, 93.6, 189.6	75.3, 75.3, 459.7	74.1, 74.1, 449.7	115.9, 115.9, 52.6
α, *β*, *γ* (°)	90, 90, 90	90, 90, 120	90, 90, 120	90, 90, 120	90, 90, 120
Resolution (Å)	50–2.67(2.81–2.67)[1]	50–2.0(2.07–2.0)	30–2.7(2.85–2.7)	30–2.79(2.94–2.79)	40–2.21(2.27–2.21)
R_{sym} or R_{merge}	0.072(0.317)	0.078(0.524)	0.061(0.636)	0.094(0.615)	0.081(0.635)
$I / \sigma I$	11.0(3.4)	30.3(2.5)	29.9(4.2)	18.9(3.3)	11.6(2.8)
Completeness (%)	97.6(96.5)	99.9(99.7)	99.5(98.6)	99.4(96.8)	99.6(100)
Redundancy	3.4(3.0)	3.8(3.4)	16.8(13.6)	19.0(13.5)	6.0(6.1)
Refinement					
Resolution (Å)	50–2.67	50–2.0	30–2.7	30–2.79	40–2.21
No. reflections	101826	63238	22290	19374	20424
R_{work} / R_{free}	0.218/0.263	0.158/0.18	0.203/0.268	0.187/0.266	0.168/0.205
No. atoms					
Protein	18693	6277	4261	4264	1820
Ligand/ion	18	6	3	3	3
Water	121	340	10	24	132
B-factors					
Protein	57.2	39.9	102.0	84.4	53.4
Ligand/ion	56.3	34.2	92.5	87.6	38.2
Water	48.4	38.0	67.5	57.9	57.3
R.m.s. deviations					
Bond lengths (Å)	0.011	0.008	0.009	0.009	0.008
Bond angles (°)	1.35	1.142	1.308	1.227	1.185

[1]Values in parentheses are for highest-resolution shell.

Table 2

Dissociation constants (K_d) for interactions between CBL variants, UbcH5B variants and ZAP-70 peptide

Immobilized Protein	Analyte	K_d (μM)[1]
GST-CBL$_{47–435}$		
WT	UbcH5B	311 ± 25
M222F	UbcH5B	320 ± 27
M222E	UbcH5B	70 ± 8
Y371F	UbcH5B	250 ± 6
Y368F	UbcH5B	138 ± 4
Y368F pY371	UbcH5B	28 ± 1
Y368F pY371 K389A	UbcH5B	81 ± 2
Y368F pY371 V431A	UbcH5B	43 ± 2
WT	UbcH5B K4A	619 ± 140
M222F	UbcH5B K4A	595 ± 120
M222E	UbcH5B K4A	225 ± 10
WT	UbcH5B + ZAP-70 peptide[2]	244 ± 7
WT	ZAP-70 peptide	17 ± 0.4
Y368F pY371	ZAP-70 peptide	11 ± 1
GST-CBL$_{354–435}$		
WT	UbcH5B	42 ± 2
pY371[3]	UbcH5B	20 ± 1
Y368F	UbcH5B	38 ± 2
Y368F pY371	UbcH5B	18 ± 1
Y371F	UbcH5B	50 ± 3

s.e.m. are indicated. Number of replicates, representative sensorgrams and binding curves are shown in Supplementary Fig. 3.

[1] Due to the weak E2 binding, we could not saturate E2 concentrations for some of these measurements. The K_d values were approximated by fitting data obtained from 0–90 μM E2 using steady state affinity analyses.

[2] Saturated ZAP-70 peptide (100 μM) was included in the analyte.

[3] This sample contained trace amounts of GST-CBL$_{354–435}$ pY368.

Table 3

Estimates of kinetic constants for CBL autoubiquitination with UbcH5B

	k_{cat} (min^{-1})	K_m (μM)	k_{cat}/K_m (min^{-1} M^{-1})
Full-length CBL			
WT[1,2]	–	–	3,400
M222E[1,2]	–	–	8,300
M222F[1,2]	–	–	3,200
WT+ZAP-70 peptide[1,2]	–	–	3,600
$CBL_{47–435}$			
WT[1,2]	–	–	190
Y371F[1,2]	–	–	200
Y368F[1,2]	–	–	387
WT[1,3]	–	–	68
pY371[3]	0.68 ± 0.07	6.5 ± 1.6	105,540
Y368F pY371[3]	0.75 ± 0.07	7.7 ± 1.4	97,260
Y368F pY371 K389A[3]	0.22 ± 0.04	17.4 ± 4.9	12,780
Y368F pY371 V431A[3]	0.13 ± 0.02	15.6 ± 3.5	8,460

Kinetic constants were determined by fitting two independent datasets onto the Michaelis-Menten equation. s.e.m. are indicated.

[1] An estimated k_{cat}/K_m was reported, because the reaction was not saturated.

[2] Reactions were performed at 30°C.

[3] Reactions were performed at 22°C.